



## Microfluidic Point-Of-Care Device for Detection of Early Strains and B.1.1.7 Variant of SARS-CoV-2 Virus

Journal:	<i>Lab on a Chip</i>
Manuscript ID	LC-ART-01-2022-000021.R1
Article Type:	Paper
Date Submitted by the Author:	08-Feb-2022
Complete List of Authors:	<p>Lim, Jongwon; University of Illinois at Urbana-Champaign, Bioengineering            Stavins, Robert; University of Illinois at Urbana Champaign, Mechanical Engineering            Kindratenko, Victoria; University of Illinois at Urbana-Champaign, Bioengineering            Baek, Janice; University of Illinois at Urbana-Champaign, Materials Science and Engineering            Wang, Leyi; University of Illinois at Urbana-Champaign            White, Karen; Biomedical Research Center, Carle Foundation Hospital            Kumar, James; Carle Foundation Hospital            Valera, Enrique; University of Illinois at Urbana-Champaign, Department of Bioengineering            King, William; University of Illinois at Urbana-Champaign, Mechanical Science and Engineering            Bashir, Rashid; University of Illinois at Urbana Champaign, Micro and Nanotechnology Laboratory</p>

# Microfluidic Point-Of-Care Device for Detection of Early Strains and B.1.1.7 Variant of SARS-CoV-2 Virus

Jongwon Lim <sup>1 a,b</sup>, Robert Stavins <sup>1 c</sup>, Victoria Kindratenko <sup>a</sup>, Janice Baek <sup>b,h</sup>, Leyi Wang <sup>d</sup>, Karen White <sup>e,f</sup>, James Kumar <sup>e,f</sup>, Enrique Valera <sup>\*a,b</sup>, William Paul King <sup>\*b,c,e,g</sup>, Rashid Bashir <sup>\*a,b,c,e,g,h,i</sup>

<sup>a</sup> Department of Bioengineering, University of Illinois at Urbana–Champaign, Urbana, IL 61801, United States

<sup>b</sup> Nick Holonyak Jr. Micro and Nanotechnology Laboratory, University of Illinois at Urbana–Champaign, Urbana, IL 61801, United States

<sup>c</sup> Department of Mechanical Science and Engineering, University of Illinois at Urbana–Champaign, Urbana, IL 61801, United States

<sup>d</sup> Veterinary Diagnostic Laboratory and Department of Veterinary Clinical Medicine, University of Illinois at Urbana-Champaign, Urbana, IL, USA

<sup>e</sup> Department of Biomedical and Translational Sciences, Carle Illinois College of Medicine, Urbana, IL 61801, United States

<sup>f</sup> Carle Foundation Hospital, Urbana, Illinois 61801, United States

<sup>g</sup> Department of Electrical and Computer Engineering, University of Illinois at Urbana–Champaign, Urbana, IL 61801, United States

<sup>h</sup> Department of Materials Science and Engineering, University of Illinois at Urbana–Champaign, Urbana, IL 61801, United States

<sup>i</sup> Carl R. Woese Institute for Genomic Biology, University of Illinois at Urbana–Champaign, Urbana, IL 61801, United States

<sup>1</sup> J.L. and R.S. contributed equally.

\*Corresponding Authors: E.V. (evalerac@illinois.edu), W.P.K. (wpk@illinois.edu), R.B. (rbashir@illinois.edu).

## Abstract

Since the beginning of the COVID-19 pandemic, several mutations of the SARS-CoV-2 virus have emerged. Current gold standard detection methods for detecting the virus and its variants are based on PCR-based diagnostics using complex laboratory protocols and time-consuming steps, such as RNA isolation and purification, and thermal cycling. These steps limit the translation of technology to the point-of-care and limits accessibility to under-resourced regions. While PCR-based assays currently offer the possibility of multiplexed gene detection, and commercial products of single gene PCR and isothermal LAMP at point-of-care are also now available, reports of isothermal assays at the point-of-care with detection of multiple genes are lacking. Here, we present a microfluidic assay and device to detect and differentiate the Alpha variant (B.1.1.7) from the SARS-CoV-2 virus early strains in saliva samples. The detection assay, which is based on isothermal RT-LAMP amplification, takes advantage of the S-gene target failure (SGTF) to differentiate the Alpha variant from the SARS-CoV-2 virus early strains using a binary detection system based on spatial separation of the primers specific to the N- and S-genes. We use additively manufactured plastic cartridges in a low-cost optical reader system to successfully detect the SARS-CoV-2 virus from saliva samples (positive amplification is detected with concentration  $\geq 10$  copies/ $\mu\text{L}$ ) within 30 min. We demonstrate that our platform can discriminate the B.1.1.7 variant (USA/CA\_CDC\_5574/2020 isolate) from SARS-CoV-2 negative samples, but also from the SARS-CoV-2 USA-WA1/2020 isolate. The reliability of the developed point-of-care device was confirmed by testing 38 clinical saliva samples, including 20 samples positive for Alpha variant (sensitivity  $> 90\%$ , specificity = 100%). This study highlights the current relevance of binary-based testing, as the new Omicron variant also exhibits S-gene target failure and could be tested by adapting the approach presented here.

## Introduction

The advent of the severe acute respiratory syndrome coronavirus 2 (SARS-CoV-2) infection in 2019 and its emergence as a global pandemic have left an unprecedented impact on global health, society, and the world economy [1]. Even though there were a small number of genetic variations at the beginning of the pandemic, the lack of herd immunity against the new pathogen, the large number of infected individuals including breakthrough infections and consequent viral spread, provided a high chance for genetic mutation and selection resulting in the accumulation of the various changes in the amino-acid sequence causing new variants [2], [3]. These SARS-CoV-2 variants originated from different parts of the world and have now spread rapidly. This spread of variants has again compromised timely access to crucial medical services due to a shortage of resources such as medical personnel, facilities, and medicine. With the significant health threat imposed by several variants, the World Health Organization (WHO) has designated five strains of variants circulating around the world as Variants of Concern (VOC): B.1.1.7 (Alpha), B.1.351 (Beta), P.1 (Gamma), B.1.617.2 (Delta), and B.1.1.529 (Omicron) [4]. One of the defining characteristics of the variants is their higher transmissibility and reproductive rates based on the increased binding affinity to human angiotensin-converting enzyme 2 (ACE2) receptors [5]. In particular, the B.1.1.7 variant, which emerged in the United Kingdom in September 2020, has spread to more than 50 countries with ~43%-90% increased transmission rate compared to preexisting variants [6]. One of its major mutations is the 69-70 deletion in the Spike gene that enables the serendipitous differential ability of the TaqPath PCR assay through the S-gene target failure (SGTF) [7]. To date, fast and highly accurate identification of the SARS-CoV-2 strains and tracking of the mutated S-gene sequence are the essential approaches to mitigating the spread of the virus. Monitoring the changing nature of the virus allows for the effective development of countermeasures against the pathogen [5], [8], [9].

To facilitate the surveillance of readily known strains for effective management of the pandemic, multiplexed real-time reverse transcription quantitative PCR (RT-qPCR) methods capable of offering single-base sensitivity have been used as a viable alternative. For example, SARS-CoV-2 single

mutation RT-qPCR Assay (Bio-Rad Laboratories, Inc.) can be used to support the detection of single or multiple mutations, and early strain sequences [10]. In another example, SARS-CoV-2 mutation detection kits (BGI Genomics) allow rapid identification of the SARS-CoV-2 B.1.1.7 lineage by detecting all 6 mutations in the S-gene region [11]. Importantly, although not specifically designed for the purpose of differentiation, the TaqPath™ COVID-19 test (ThermoFisher Scientific) is being widely used to identify variant B.1.1.7 with a negative or significantly weaker positive S-gene result (also called S-gene target failure, SGTF) while diagnostic accuracy is maintained using the built-in redundancy with simultaneous detection of two other genes (ORF1ab- and N-gene) [12]. Interestingly, from a multiplexing point of view, Xpert Xpress CoV-2/Flu/RSV plus (Cepheid) allows the multiplexed detection of the SARS-CoV-2 virus, as well as other similar symptom viruses such as Flu A, Flu B, and RSV in 25 min. This test has recently been approved for emergency use by the U.S. Food and Drug Administration [13]. However, introduced assays and other techniques based on the RT-qPCR methods are time-consuming (2~4 h), require specialized benchtop equipment such as a thermocycler and, depending on the degree of automation of the instrument, could also require a trained technician to perform the laborious extraction and purification steps [1], [14]–[16]. These same characteristics make it difficult for the RT-qPCR technique to be used in under-resourced areas with lacking laboratory settings. Moreover, the shortage of reagents due to repetitive tests make RT-qPCR unable to meet the high demands of diagnostic tests [1], [17]–[19]. These limitations highlight the necessity of developing alternative techniques that can facilitate the development of point-of-care (POC) devices that enable simple, portable, and cost-effective solutions for the detection and differentiation of SARS-CoV-2 variants [1].

Reverse transcription loop-mediated isothermal amplification (RT-LAMP) is an attractive alternative to PCR-based assays, especially for its application in devices intended to be used at the point-of-care. Being an isothermal technology, RT-LAMP does not require thermocycling, which results in cost-effective, portable hardware while maintaining assay sensitivity and specificity [1], [20]. Additionally, RT-LAMP performs well with crude samples thanks to the robustness of Bst DNA polymerase [21]. The advantages of using RT-LAMP in the development of molecular POC devices can be further

enhanced by using a simple thermal lysis step to release genetic material, thus avoiding time-consuming purification steps and increasing the cost of the assay [22], [23]. Due to these numerous advantages, RT-LAMP has recently gained attention for the development of POC devices intended for the detection of the SARS-CoV-2 virus [1], [20], [24]. Importantly, some point-of-care isothermal amplification-based technologies such as ID NOW COVID-19 (Abbott Diagnostics Scarborough, Inc) [25], Cue COVID-19 Test (Cue Health) [26], and Lucira COVID-19 All-in-One Test Kit (Lucira Health, Inc.) [27] have received EUA FDA approval and are commercially available. Furthermore, the Cue COVID-19 and Lucira COVID-19 All-in-One tests have received authorization for non-prescription home use. However, to the best of our knowledge, to date there are no studies reporting the use of RT-LAMP in a POC device for the detection and differentiation of multiple genes and variants of the SARS-CoV-2 virus.

In this paper, we have combined RT-LAMP isothermal amplification with additive manufacturing (AM) technology and a smartphone-based optical reader to develop a multiplexed POC platform that can detect and differentiate the SARS-CoV-2 virus (USA-WA1/2020 isolate) and the Alpha variant from the same human saliva sample. An extensive validation of the developed multiplexed POC system was carried out, which included the analysis of human saliva from healthy donors spiked with inactivated SARS-CoV-2 virus standards (USA-WA1/2020 and USA/CA\_CDC\_5574/2020 isolates) and the analysis of 38 clinical saliva samples. Of these 38 clinical samples, 11 samples were positive for sequence representative of isolates of SARS-CoV-2 circulating early in the pandemic, 20 samples were positive for the Alpha variant, and 7 samples were negative. All were confirmed by RT-qPCR analyses. In addition, the platform developed in this work was used not only for the detection of B.1.1.7 variant clinical saliva samples, but also for their differentiation from negative samples, as well as from samples from isolates of SARS-CoV-2 circulating early in the pandemic. Importantly, the new Omicron variant also exhibits the S-gene target failure [28], hence, this device could also be applied for the detection and differentiation of the Omicron variant from other isolates with the appropriate use of primers.

## **Materials and Methods**

### **Inactivated SARS-CoV-2 virus**

Gamma-Irradiated SARS-Related Coronavirus 2 (Isolate USA-WA1/2020, NR-52287), and Heat-inactivated (B.1.1.7) SARS-Related Coronavirus 2 (Isolate USA/CA\_CDC\_5574/2020, NR-55245), were obtained from the BEI Resources, aliquoted in small volumes (2  $\mu$ L), and stored at  $-80^{\circ}\text{C}$  until further use. For experiments, serial dilutions of the stock concentration were performed in human saliva (pooled human donors collected before November 2019, Lee Biosolutions, Cat# 991-05-P-PreC), followed by thermal lysis ( $95^{\circ}\text{C}$ , 10 minutes). Afterwards, samples were mixed with TE buffer (5% Tween 20, 1:1 ratio). The thermal lysis step was applied to all samples in the same manner including negative and positives clinical saliva samples.

### **Clinical samples**

Saliva clinical samples were collected: 1) from in-patients at Carle Foundation Hospital (Urbana, IL) who had tested COVID-19 positive (RT-qPCR) when they were admitted to the hospital (for at most 14 days before admission), after the administration of informed consent, through an approved institutional review board (Carle IRB # 20CRU3150); and 2) as part of the COVID detect study through an approved IRB (WIRB® Protocol #20202884, all participants provided informed consent).

For saliva samples from Carle Hospital, after consent, the subjects were asked to let their saliva pool in their mouth and then to open their mouth and let the saliva fall/dribble into the collection tube. At the same time as the saliva collection, nasal swab samples were also collected from the same subject at Carle Foundation Hospital and analyzed by the RT-qPCR technique at the Carle clinical lab. A total of 18 deidentified samples were received either fresh (during the collection day) or frozen (the next day after the collection day). For samples from the COVID detect study at UIUC, we received 20 positive frozen samples (confirmed B.1.1.7 variant, 100  $\mu$ L/each) and RT-qPCR Ct values. The sample collection protocol is detailed in [29].

### **Primer sequences**

RT-LAMP primers sequences were designed using New England Biolabs® (NEB) LAMP primer design tool and synthesized by Integrated DNA Technologies. Genome assembly was conducted using the Snapgene software by mapping to the SARS-CoV-2 reference genome (NCBI accession number NC\_045512.2 and MW981411.1, respectively for Wuhan-Hu-1 and SARS-CoV-2/human/USA/CA\_CDC\_5574/2020 isolates). Three primer sets were used in the paper. Two of them, against N- and S-genes from the early strains, were previously developed by our group [20], and successfully detected with virus concentrations  $\geq 10$  copies/ $\mu\text{L}$  (supplementary information, **Figure S1**). The third primer set is against the S-gene and specific for detecting the S-gene target failure against 69-70 deletion in the Alpha variant, see **Results** section.

### **RT-LAMP detection assay**

The preparation of the RT-LAMP reaction mix begins with the preparation of the buffer mix from the following items:  $\text{MgSO}_4$  (4 mM, NEB), isothermal amplification buffer (1 $\times$  final concentration, NEB), deoxyribonucleoside triphosphates (dNTP, 1.025 mM each), and Betaine (0.29 M, Sigma-Aldrich). Individual reagents were stored properly according to the manufacturer's instructions. The second step is to add the following ingredients into the freshly made buffer mix: bovine serum albumin (1 mg/mL, NEB), EvaGreen (0.735X, Biotium), Bst 2.0 WarmStart DNA polymerase (0.47 U/ $\mu\text{L}$ , NEB), WarmStart reverse transcriptase (0.3 U/ $\mu\text{L}$ , NEB), primer mix (0.15  $\mu\text{M}$  of F3 and B3, 1.17  $\mu\text{M}$  of forward inner primer (FIP) and BIP, and 0.59  $\mu\text{M}$  of LoopF and LoopB). The rest of the volume was filled with nuclease-free water. In the case of the on-cartridge experiments with two detection reservoirs, the primers were not included in the reaction mix but were dried directly on the cartridge (23°C, 30% humidity, 20 min) [30].

For the detection of variant B.1.1.7, a guanidine hydrochloride solution (GnCl, 11 mM, pH ~8, Sigma-Aldrich) was added to RT-LAMP reaction mix. Thus, 75% of the nuclease-free water was substituted by GnCl.

For the off-cartridge assays, thermally lysed saliva samples (2  $\mu\text{L}$ ) and RT-LAMP reaction mix (14  $\mu\text{L}$ )

were mixed in 0.2 mL PCR tubes. RT-LAMP amplification was conducted in the QuantStudio 3 system (Applied Biosciences) at 65°C for 50 minutes with three repeats per sample. Fluorescence data were measured and recorded every 1 minute. Normalization of the raw fluorescence data was carried out and the amplification threshold time was decided based on when 20% of the normalized fluorescence threshold was reached.

### **RT-qPCR control assays**

TaqPath™ COVID-19 Combo Kit (ThermoFisher Scientific) was used to perform the RT-qPCR control assays. Reagents were stored following the manufacturer's instructions. The RT-qPCR master mix consisted of: TaqPath Multiplex 1-step Master Mix (200 µL, no ROX), Primer/Probe mix (40 µL), and nuclease-free water (160 µL). For the RT-qPCR assay, thermally lysed samples (5 µL) were mixed with the RT-qPCR master mix (5 µL). The assays were performed in 0.2 mL PCR tubes in a QuantStudio 3 system with the following thermal cycling steps: 25°C, 2 minutes; 53°C, 10 minutes; 95°C, 2 minutes; 40 cycles of 95°C, 3 seconds; and 60°C, 30 seconds.

### **Additively manufactured cartridge**

The cartridge material is rigid polyurethane 70 (RPU-70) and was fabricated using the Carbon M2 printer. The print orientation for this part was with one of the long, thin sides on the build tray. Post-processing fabrication included wash and cure steps. Prior to use, each cartridge was washed and dried again with compressed air, then the back side was sealed with transparent biocompatible tape (ARSeal 90880, Adhesive Research) and a syringe needle was connected. The cartridge design was split into four major functional regions: the inlet, mixing region, detection regions, and pull port. The inlet is a unified inlet for both the prepared sample and RT-LAMP reaction mix. The inlet is connected to the 3D micromixer with a single rectangular channel that is 0.7 mm wide, 0.4 mm deep, and 22.5 mm long. The 3D micromixer consists of serpentine channels, where the fluid goes between the top and bottom faces after each serpentine turn. The mixer has two columns of 5 stacked serpentes, with each microchannel being 0.7 mm wide, 0.4 mm deep, and 10.5 mm long. From the mixer, the fluid travels to the detection region where there is a Y-junction to split the mixed sample and reagents into the two

rectangular detection regions. Each detection region is 2 mm wide, 2 mm deep, and 5.5 mm long. On the opposite side of the rectangular regions the channels are 0.5 mm wide by 0.4 mm deep. This constriction allows both detection regions to be filled before any fluid spills over. Also included in the detection region are two circular wells with diameter of 3.5 mm and depth of 2 mm which serve as control regions than can be loaded separately with positive and negative biological controls as labeled. The final region is the pull port where the external pulling mechanism, a 1 mL syringe, is connected via tubing. Both the pull port and the inlet ports have raised circular geometries that are snap-in mates with corresponding caps for cartridge sealing purposes. The caps are fabricated from RPU-130, a softer material than RPU-70. For the pull port there is an additional elastic polyurethane (EPU) stopper plug inserted. The putty we used is a multi-purpose quick setting putty (Loctite, 1999131). The sealing geometry can be seen in **Figure S2** (supplementary information). Mixing characterization through the AM cartridge can be found in supplementary information (**Results 1**).

### **Cradle fabrication**

The disposable cartridge interfaces with a reusable POC reader shown in **Figure S3** (supplementary information). We used a smartphone (Google Pixel 5, Google) to detect the fluorescence emission from on-cartridge amplification. The top part of the reader holds the smartphone and aligns its camera with an optical array consisting of a macro lens (12.5 $\times$ , Techo-Lens-01, Techo) and a long-pass filter (525 nm, 84-744, Edmund Optics). The macro lens enables close-up imaging ( $\sim$ 50 mm imaging distance) and the long-pass filter allows only the light from the EvaGreen dye to reach the camera. The reader also encases a printed circuit board (PCB) and filter holder. The PCB has an array of eight LEDs ( $\lambda_{\text{peak}} = 485$  nm, XPEBBL, Cree) arranged in a circular configuration to illuminate the detection and amplification regions of the cartridge. The LEDs are lined up with four short-pass filters (490 nm, 490 RapidEdge, Omega Filters). A positive temperature coefficient (PTC) heater (12 V-80 $^{\circ}$ C, Uxcell) is housed in the reader to act as the isothermal heat source for the RT-LAMP reaction. Finally, there is a magnetic clamping system consisting of large neodymium magnet embedded in the bottom of the reader and a smaller neodymium magnet that rests on top of the cartridge to provide better contact between

the cartridge and the heater. The smaller magnet is positioned such that there is no interference with the fluorescent imaging.

### **On-cartridge detection assay and analysis**

In the case of the on-cartridge detection with a single detection reservoir, thermally lysed sample (6  $\mu\text{L}$ ) and RT-LAMP reaction mix (42  $\mu\text{L}$ ) were loaded into the inlet region of the microfluidic cartridge (supplementary information, **Figure S4A**). For the multiplexed on-cartridge detection with two detection reservoirs, primer dehydration was accomplished by adding multiple 5  $\mu\text{L}$  drops of each primer set (each set separated in a separate reservoir) prior to sealing the cartridge. After sealing the cartridge with transparent tape, thermally lysed sample (7  $\mu\text{L}$ ) and RT-LAMP reaction mix (49  $\mu\text{L}$  without including the primers) were loaded into the inlet region of the cartridge. Then, the loaded reagents were pulled through the three-dimension (3D) serpentine using the syringe connected to the pull port. After the solution completely filled the two detection reservoirs, the inlet and outlet ports were sealed to avoid potential contamination issues. Afterward, the cartridge was inserted into the cradle over the internal heater (set to 65°C). After 5 minutes of thermal stabilization, fluorescence images were taken every 5 minutes using the smartphone (settings: ISO 500, exposure time = 0.5 seconds).

For experiments with inactivated virus, image analysis was conducted using the ImageJ (<https://imagej.nih.gov/ij/>) software by selecting 4 random points and averaging four fluorescence data. For experiments with clinical samples, a Python program was developed to reduce the external errors that may be caused by arbitrarily selected data points. Images were loaded using the Python Image Library (PIL), which allows for basic image-manipulation operations. Next, we set up the rectangles which define the area of interest in the images. RGB pixel values were extracted over the specified area by moving from one pixel to another, accumulating the RGB values for each pixel and counting the number of pixels encountered. At the end, the average intensity value was calculated for each rectangle of interest in each image for each color channel which were then recorded into an array. The normalized fluorescence values are fitted to a sigmoidal curve for smoothing the amplification curve.

For the Receiver Operating Characteristic (ROC) curve analysis, Wilson/Brown method was used, and

the ROC curve was reported as a percentage, based on 95% confidence intervals. Subsequently, an informational table regarding the Area Under the Curve (AUC) and p-value for each time point was shown for each ROC figure.

For t-test analysis, unpaired and two-tailed t-test with 95% confidence level was conducted by assuming both populations have the same standard deviation.

## **Results**

### ***Schematic workflow***

The complete workflow, from sample collection to optical detection, is shown in **Figure 1A**, and described in the *On-cartridge detection assay and analysis* section. In the protocol, the lysed sample is mixed with TE buffer (5% Tween 20), as this buffer has demonstrated to improve sensitivity of the assay [22] while simultaneously diluting the sample by reducing saliva viscosity [31]. Once the mixture enters the amplification-detection reservoirs, both the inlet and outlet of the microfluidic cartridge are sealed using putty and caps. The temperature of the RT-LAMP amplification can result in movement of the solution in the cartridge. Thus, the sealing of the soft cap is improved by adding the putty as a secondary sealing method. During the amplification reaction, a smartphone is used as the device display to monitor and record changes in fluorescence as explained in the *Materials and Methods* section.

### ***Development of the primer sets***

The developed multiplexed POC device can not only indicate whether the saliva sample is SARS-CoV-2 negative or positive, but also distinguish a mutated virus (B.1.1.7) from SARS-CoV-2 lineages from earlier in the pandemic that didn't have that dropout sequence. This differentiation is possible using RT-LAMP primers specifically designed to detect amino acids 69 and 70 located in the N-terminal domain of the S1 spike fragment (S gene). These amino acids are deleted in the Alpha variant [32], which causes the SGTF effect when the S-gene is analyzed the Alpha variant samples.

The binary detection method developed in this paper uses: 1) RT-LAMP primers against the N-gene to target regions of the virus sequence that are homologous and conserved across the Alpha variant and

the SARS-CoV-2 virus early strains; and 2) RT-LAMP primers against the S-gene to target amino acids 69 and 70 which are expressed in the early SARS-CoV-2 virus strains but not in the Alpha variant. To design the primers against the S-gene, the 5' end of F1c or B1c are required to be in the amino acids 69 and 70, so that initial strand displacement by either forward or backward inner primer does not happen. In addition, this primer design method prevents stem loop DNA structures, which are essential for the exponential amplification, from being created even under the presence of mutated RNA sequence. As a result, the RT-LAMP reaction would not occur despite the presence of the variant sequence since the essential primer cannot start the exponential amplification due to lack of its hybridization with the target region. The decision criteria to distinguish the Alpha variant from the early SARS-CoV-2 virus strains using the binary detection method can be seen in **Table S1** (supplementary information). The RT-LAMP primers for the SGTF (**Figure 1B**) show that the 5' of F1c is targeting the 69-70 deletion region so that the exponential amplification process does not happen if the B.1.1.7 variant sample is introduced.

### ***Multiplexed on-cartridge detection***

To provide the developed device with multiplexing capabilities, two detection reservoirs were included in the cartridge (**Figure 1A**) and specific primer sets were not included in the reaction mix but were pre-dried and physically separately in the two detection reservoirs (**Video S1**).

Representative examples of the real-time amplification images obtained using the POC platform for multiplexed on-cartridge detection can be seen in **Figure 2A**. Two concentrations ( $10^4$  and 10 copies/ $\mu\text{L}$ ) of the SARS-CoV-2 USA-WA1/2020 isolate were spiked in healthy human saliva. Likewise, inactivated SARS-CoV-2 USA-WA1/2020 isolate concentrations, in the range from  $10^4$  to 0 copies/ $\mu\text{L}$ , were spiked in human saliva and tested using the platform. **Figures 2B-C** show the normalized fluorescence data, for the N- and S-gene, respectively. From the normalized data, the amplification threshold times were calculated at 20% of the maximum intensity (denoted as the pink dotted line) and plotted in **Figure 2D**. While negative controls did not show amplification and amplification curves, positive amplification was seen in all trials for concentrations  $\geq 10$  copies/ $\mu\text{L}$  for both target genes. Calibration curves for the detection of SARS-CoV-2 USA-WA1/2020 isolate spiked in saliva can be

seen in **Figure 2E** for the N ( $y = -3.6x + 26.5$ ,  $R^2 = 0.64$ ) and S ( $y = -4.5x + 32.6$ ,  $R^2 = 0.70$ ) genes. In addition to the multiplexed on-cartridge detection, we also tested adding a negative control reservoir in the microfluidic cartridge (**Figure S5**). The negative control was performed by adding a reaction mix and negative control sample (human saliva from healthy donors). As shown in **Figure S5**, there was no amplification in the negative control region (highlighted with the white box) while the SARS-CoV-2 genes showed reliable amplification, demonstrating the ability to include a negative control as a side assay.

Characterization of the off-cartridge and on-cartridge single assay were included in the supplementary information (**Results 2** and **Results 3**).

#### ***Multiplexed on-cartridge detection of SARS-CoV-2 early strains from clinical saliva samples***

Before on-cartridge testing, the clinical saliva samples were tested off-cartridge and results were compared with RT-qPCR gold standard technique (**Results 4**, supplementary information).

The multiplexed on-cartridge POC device was validated by testing 18 clinical saliva samples (Carle Foundation Hospital). For details on experimental protocols, see the *Methods* section. **Figure 3A** summarizes the fluorescence intensities and amplification threshold time results obtained from the on-cartridge detection of the clinical samples. From the 18 samples, 11 samples were confirmed positives and 7 samples were confirmed negative for SARS-CoV-2 early strains by the RT-qPCR technique. When comparing our on-cartridge results with the RT-qPCR control, the 7 confirmed negative samples did not amplify, and 10 out of 11 of the confirmed positive samples were detected as positives with the developed device (**Figure S6**, supplementary information). The one positive sample that did not amplify with the developed device (S3) showed a high Ct value ( $> 33$  for N-gene) in the RT-qPCR analysis. Thus, our multiplexed on-cartridge device showed 91% sensitivity (95% confidence interval (CI) is 59% -99.8%) and 100% specificity (95% CI is 59% - 100%). Next, ROC curves were plotted for N- and S-genes at different amplification time points (**Figures 3B-C**) to determine the amplification threshold time. The Area Under the Curve (AUC) and related p-values were also calculated for different amplification times. Since the AUC values were saturated after 30 minutes, we decided to use the data

sets at 30 minutes for establishing a discerning criterion for differentiating positive from negative samples (**Figures 3D-E**). In these figures the results obtained from the clinical samples were compared with a created baseline (using 6 known negatives samples). Samples with fluorescence intensity above the average of the baseline plus 3 times the standard deviation ( $3\sigma$ ) of the average were considered as positive, while samples with fluorescence intensity below the average of the baseline plus  $3\sigma$  of the average were considered as negative. The average and  $\sigma$  were calculated using the fluorescence difference between the starting point (0 min) and the end point (30 min) of amplification. Normalized and raw fluorescence intensities of 18 clinical samples during the amplification time for N- and S-genes can be found in **Figures S7A-D** (supplementary information). As a result, all samples but S3 (specified with an arrow in **Figures 3D-E**) were successfully categorized into the correct groups. In addition, t-test statistical analysis was performed between positive and negative samples at different time points to determine confirmation between positive and negative samples, (**Figures S7E-F**, supplementary information).

Characterization of the off-cartridge and on-cartridge single assay were included in the supplementary information (**Results 2** and **Results 3**).

#### ***Assay validation for detection of SARS-CoV-2 (B.1.1.7 variant) from clinical saliva samples***

We also assessed the ability of the multiplexed POC device to distinguish the SARS-CoV-2 B.1.1.7 variant from early SARS-CoV-2 strains and from negative samples. For this purpose, we first characterized the off-cartridge RT-LAMP assay using the new S-gene primer specific to detect the SGTF. **Figures S8A-D** (supplementary information) shows the normalized fluorescence intensities, and the amplification threshold times for the SARS-CoV-2 early strains and for the SARS-CoV-2 B.1.1.7 variant. In the case of the primer set against the N-gene, both the SARS-CoV-2 early strains and the B.1.1.7 variant showed proper amplification with an observation of positive amplification in all trials when starting with  $\geq 10$  copies/ $\mu\text{L}$ . On the other hand, the SGTF-specific primer set specific demonstrated the ability to detect target failure by lacking amplification in the S-gene for any virus concentrations in the range from 10 to  $10^4$  copies/ $\mu\text{L}$ . However, the S-gene primer specific to detect the

SGTF showed amplification for concentrations  $\geq 10^3$  copies/ $\mu\text{L}$  for the SARS-CoV-2 USA-WA1/2020 isolate, meaning the assay may not be able to detect the SARS-CoV-2 early strains correctly in samples with low viral load. To improve the sensitivity of the assay, GmCl was added to the reaction mix, as GmCl has been reported to increase the speed and sensitivity of the colorimetric LAMP reaction [33]. As can be seen in **Figures S8E-F** (supplementary information) and **Figure 4A**, after adding GmCl in the reaction the N-gene was successfully detected with virus concentrations  $\geq 10$  copies/ $\mu\text{L}$ , but with faster amplification time for both SARS-CoV-2 USA-WA1/2020 and SARS-CoV-2/human/USA/CA\_CDC\_5574/2020 isolates. In the case of the S-gene, the lowest concentration with all trials amplifying well for the SARS-CoV-2 USA-WA1/2020 isolate was  $10^2$  copies/ $\mu\text{L}$  (1/3 replicates of 40 copies/ $\mu\text{L}$  amplified) while maintaining the SGTF ability for the variant detection (**Figure S8G-H**, supplementary information). **Figure S9** (supplementary information) summarizes the improved sensitivity of the assay when GmCl was included in the reaction mix. Next, the 20 clinical saliva samples (confirmed to be B.1.1.7 variant positives by the RT-qPCR assay) were analyzed with the improved RT-LAMP assay. In the RT-qPCR assay the N- and Orfla-genes of those 20 variant samples amplified while the S-gene did not show any amplification, indicating the S-gene target failure (**Figure S10**, supplementary information). When these samples were tested with the improved off-cartridge RT-LAMP assay, none of the S-gene amplified when using the S-gene primers specific for detecting the target failure (**Figures S10A and S10C**, supplementary information). Likewise, the 20 samples confirmed N-gene positive by RT-qPCR were also positives with our RT-LAMP assay. Out of the 20 samples, 17 samples had all three replicates amplify. In the case of the positive sample V7, 2/3 replicates amplified and for samples V11 and V15, 1/6 replicates amplified (amplification time = 40 min. and 43 min. respectively).

#### ***Multiplexed on-cartridge detection of SARS-CoV-2 (B.1.1.7 variant) from clinical saliva samples***

We also assessed the isothermal multiplexed POC platform to distinguish three clinical sample groups: negative samples, SARS-CoV-2 early strains samples, and B.1.1.7 variant SARS-CoV-2 samples. For this assessment 26 clinical saliva samples were tested: 20 confirmed positive for SARS-CoV-2 B.1.1.7

variant, 3 confirmed negative, and 3 of them confirmed positive for SARS-CoV-2 early strains. **Figure 4B** illustrates the differentiation criteria by reporting the binary amplification results specific to N- and S-genes. The amplified and brightened reservoir is labeled as 1 and the non-amplified reservoir is labeled as 0. Thus, (0,0), (1,1) and (1,0) of binary fluorescence results were depicted for negative, SARS-CoV-2 early strains, and B.1.1.7 variant samples, respectively (**Table S1**, supplementary information). Amplification curves of these on-cartridge analyses can be seen in **Figure S11A-F** (supplementary information). **Figure 4C** summarizes the differentiation ability of the multiplexed POC RT-LAMP device. While all confirmed SARS-CoV-2 early strains samples tested (WT 1-3) showed N- and S-gene amplification (blue and red bars), all confirmed B.1.1.7 variant samples (V 1-20) did not show amplification for the S-gene (red bar). However, only 18/20 of the confirmed B.1.1.7 variant samples showed amplification for the N-gene. Thus, two confirmed positive variant samples were detected as negative in our POC system. These results can be also appreciated in the raw fluorescence data (**Figures 11G-H**, supplementary information), statistical comparison analysis (**Figures 4D-E**) and ROC curve analysis (**Figures 4F-G**). For N-gene analysis, statistical comparison and ROC curve analysis were conducted by comparing the 20 variant samples with the 3 confirmed negative samples. For the S-gene analysis, on the other hand, the comparison between 20 variant samples and 3 SARS-CoV-2 early strains samples was performed. In both N- and S-gene assays, the p-value between the two groups was calculated to be less than 0.0029 after 30 min. of amplification. Moreover, since AUC values saturated after 30 minutes in both ROC analysis (**Figures 4F-G**), we decided to use the data sets at 30 minutes to establish a discerning criterion for differentiating negative, SARS-CoV-2 early strains, and B.1.1.7 variant samples (**Figures 4H-I**). In the N-gene assay (**Figure 4H**), all B.1.1.7 variant samples but V11 and V15 (specified with an arrow) were successfully differentiated from negative samples by showing increased fluorescence. In **Figure 4I**, all variant samples were distinguished from the SARS-CoV-2 early strains through the S-gene target failure. Therefore, reducing the detection time from 50 minutes to 30 minutes did not compromise the sensitivity or specificity of the developed assay. As a result, we were not only able to detect the B.1.1.7 variant, but also differentiate it from the SARS-CoV-2 early strains within 30 minutes of reaction time.

## Discussion

This paper demonstrates a multiplexed microfluidic POC device for the detection of SARS-CoV-2 virus (SARS-CoV-2 early strains and B.1.1.7 variant) from saliva samples. Although we previously reported on the rapid and portable detection of SARS-CoV-2 from Viral Transport Media (VTM) samples [20], that previous work was limited to the analysis of the N-gene from VTM samples. In this work we have not only expanded our approach by bringing multiplexing capabilities to the device, but also introduced a new set of RT-LAMP primers to detect the S-gene target failure in Alpha variant samples and used saliva patient samples in the additively manufactured cartridges. AM technology has significant cost advantages over injection molding in the range of several hundred thousand parts as the AM process does not require the expensive tooling needed for molding [34]. Likewise, AM technology can be used for the rapid creation of prototypes allowing for the development of working solutions in a few weeks [35]. Our approach, when combined with mass-production, is expected to be scalable so that it can reduce the overall cost of sample collection, testing, and analysis.

One of the current methods to detect and differentiate the B.1.1.7 variant from other mutations is based on the analysis of the S-gene target failure using the gold standard RT-qPCR technique. However, this method relies on the use of multiple fluorescence dyes as reporters and on benchtop thermocyclers to achieve the multiplexed detection of three genes. In contrast, our microfluidic cartridge system achieved the detection and differentiation of this variant using a single reporter by using a binary detection system based on the spatial separation of the primers specific against the N- and S-genes and using a portable and miniaturized device.

Examples of point-of-care detection of B.1.1.7 variant can be also found in the literature [36]. This interesting CRISPR-based POC diagnostic platform extracts, purifies, and concentrates viral RNA from 2 mL of unprocessed saliva. In contrast, our POC system did not require RNA concentration, used microfluidic cartridges to work with reduced volumes of sample, and achieved high specificity avoiding the use of CRISPR technology.

Using the presented device, we found 17/18 samples (SARS-CoV-2 early strains) and 18/20 samples (B.1.1.7 variant) in agreement with the RT-qPCR control without any false positives. The samples that were not detected with our assay showed high Ct values ( $> 34$ ) and hence low viral loads, and ambiguous results (not all replicates amplified) in the RT-qPCR control (**Figures S6A** and **S10A**, supplementary information). Based on a small number of observations, the condition most likely to produce false negatives for LAMP is when measuring samples with high Ct values.

Interestingly, from the SARS-CoV-2 early strains saliva samples, four of samples confirmed as positives by the VTM RT-qPCR control were detected as negatives by the saliva RT-qPCR control and by our RT-LAMP assay (**Table S2**, supplementary information). The reason for this discrepancy is most likely related to the fact that the VTM RT-qPCR control measurements included the RNA extraction/purification step, whereas the saliva RT-qPCR assay and the RT-LAMP assay did not. While this additional step can certainly provide some additional sensitivity, it not only increases the cost of the assay, but also makes the assay more susceptible to limitations in the supply chain. The comparison of our technology with other methods reported in the literature for the detection of the SARS-CoV-2 virus can be found in **Table S3**, (supplementary information).

While this paper demonstrated the platform for the detection of SARS-CoV-2 virus (early strains and B.1.1.7 variant), our system can be easily scaled either for detecting other pathogens or for distinguishing the prevalent VOC variants by simply adding the specific primers in additional chambers. These additional multiplexing capabilities can be added to our platform by changing the geometry of the microfluidic cartridge without affecting the cost of cartridge or cost of reagents, compared to running parallel reactions.

It is also relevant to emphasize that the new Omicron variant also exhibits the S-gene target failure. Therefore, the developed device here could also be applied for detection and differentiation of the Omicron variant from other isolates if the correct primers are available. However, to distinguish Alpha from Omicron variant, RNA sequencing would be necessary.

## **Conclusion**

While next generation sequencing or multiplex RT-qPCR for the surveillance of emerging SARS-CoV-2 variants are available, laboratory-based processes including RNA isolation, purification, library prep, and other time-consuming operations and labor-intensive approaches makes it difficult to rapidly track and manage viral mutations. There is an urgent need for the development of portable and rapid diagnostic devices that can detect and distinguish variants from other existing strains and that can bring rapid and inexpensive virus detection to under-resourced regions. Here, we developed a multiplexed point-of-care device for the sensitive and specific detection of the B.1.1.7 variant and its differentiation from SARS-CoV-2 early strains with saliva as the specimen. This paper demonstrated the use of LAMP isothermal amplification for the simultaneous detection of the N- and S-gene to differentiate between the SARS-CoV-2 early strains and variant on an additively manufactured cartridge and an optical reader in a low-cost, portable cradle that can be used at the point-of-care.

## **Authors contributions**

J.L., R.S., E.V., W.P.K., and R.B. designed assay and diagnostics study; E.V., K.W., J.K., and R.B. designed clinical sample collection protocols. J.L., R.S., V.K., J.B., and L.W. performed research; J.L., R.S., E.V., W.P.K., and R.B. contributed new reagents/analytic tools; J.L., R.S., V.K., L.W., E.V., W.P.K., and R.B. analyzed data; J.L., R.S., V.K., L.W., E.V., W.P.K., and R.B. wrote the manuscript.

## **ACKNOWLEDGMENTS.**

R.B., W.P.K and E.V. acknowledge support from the Foxconn Interconnect Technology sponsored Center for Networked Intelligent Components and Environments (C-NICE). R.B. and E.V. acknowledge the support of NSF Rapid Response Research (RAPID) grant (award 2028431). Microfluidic diagnostic cartridges were provided by Fast Radius Inc. The authors thank the staff at the Holonyak Micro and Nanotechnology Laboratory at UIUC for facilitating the research and the funding from University of Illinois. We also thank Mary Ellen Sherwood, Reubin McGuffin, and Carly Skadden of Carle Foundation Hospital (Urbana, IL) for their support of the IRB # 20CRU3150 and patient sample

acquisition for this study. This study was approved by the Carle Institutional Review Board, and all participants provided informed consent. The following reagent was obtained through BEI Resources, NIAID, NIH: SARS-Related Coronavirus 2, Isolate USA-WA1/2020, Gamma-Irradiated, NR-52287, contributed by the Centers for Disease Control and Prevention. The following reagent was deposited by the Centers for Disease Control and Prevention and obtained through BEI Resources, NIAID, NIH: SARS-Related Coronavirus 2, Isolate USA/CA\_CDC\_5574/2020, Heat Inactivated, NR-55245. The analyses described in this publication were conducted with samples and viral genomic data accessed through the COVID detect study. The COVID detect study was funded by the National Heart, Lung, and Blood Institute at the National Institutes of Health [3U54HL143541-02S2] as a subaward from UMass Medical School to the University of Illinois Urbana-Champaign. This study was approved by the Western Institutional Review Board, and all participants provided informed consent. Likewise, R.B., E.V., and J.L. thank Gill Snyder and Prof. Chris Brooke for their support to provide the samples from the COVID detect study.

**Conflicts of interest**

W.P.K. is a cofounder and Chief Scientist at Fast Radius Inc., where the additively manufactured cartridge was produced. The research was conducted in compliance with the conflict of interest policies at Fast Radius and University of Illinois Urbana-Champaign.

## References

- [1] E. Valera *et al.*, “COVID-19 Point-of-Care Diagnostics: Present and Future,” *ACS Nano*, vol. 15, no. 5, pp. 7899–7906, 2021, doi: 10.1021/acsnano.1c02981.
- [2] C. E. Gómez, B. Perdiguero, and M. Esteban, “Emerging sars-cov-2 variants and impact in global vaccination programs against sars-cov-2/covid-19,” *Vaccines*, vol. 9, no. 3, pp. 1–13, 2021, doi: 10.3390/vaccines9030243.
- [3] E. Boehm, I. Kronig, R. A. Neher, I. Eckerle, P. Vetter, and L. Kaiser, “Novel SARS-CoV-2 variants: the pandemics within the pandemic,” *Clin. Microbiol. Infect.*, vol. 27, no. 8, pp. 1109–1117, 2021, doi: 10.1016/j.cmi.2021.05.022.
- [4] World Health Organization, Tracking SARS-CoV-2 variants, <http://www.who.int/en/activities/tracking-SARS-CoV-2-variants/>, (Accessed, Jan 2. 2022).
- [5] R. N. Tasakis *et al.*, “SARS-CoV-2 variant evolution in the United States: High accumulation of viral mutations over time likely through serial Founder Events and mutational bursts,” *PLoS One*, vol. 16, no. 7 July, 2021, doi: 10.1371/journal.pone.0255169.
- [6] N. G. Davies *et al.*, “Estimated transmissibility and impact of SARS-CoV-2 lineage B.1.1.7 in England,” *Science (80-. )*, vol. 372, no. 6538, p. eabg3055, 2021, doi: 10.1126/science.abg3055.
- [7] C. B. F. Vogels *et al.*, “Multiplex qPCR discriminates variants of concern to enhance global surveillance of SARS-CoV-2,” *PLoS Biol.*, vol. 19, no. 5 May, pp. 1–12, 2021, doi: 10.1371/journal.pbio.3001236.
- [8] H. Wang *et al.*, “Mutation-specific sars-cov-2 pcr screen: Rapid and accurate detection of variants of concern and the identification of a newly emerging variant with spike 1452r mutation,” *J. Clin. Microbiol.*, vol. 59, no. 8, 2021, doi: 10.1128/JCM.00926-21.
- [9] Y. Wang *et al.*, “Detection of SARS-CoV-2 and Its Mutated Variants via CRISPR-Cas13-Based Transcription Amplification,” *Anal. Chem.*, vol. 93, no. 7, pp. 3393–3402, 2021, doi: 10.1021/acs.analchem.0c04303.
- [10] Bio-Rad, ddPCR and RT-PCR Assays for SARS-CoV-2 Variant Surveillance, <https://www.bio-rad.com/featured/en/sars-cov-2-variants-pcr-assays.html>, (Accessed, Jan 2. 2022).
- [11] BGI, SARS-CoV-2 Variant Identification Panel, <https://www.bgi.com/us/sars-cov-2-variant-detection/>, (Accessed, Jan 2. 2022).
- [12] Thermo Fisher Scientific, The S Gene Advantage: TaqPath COVID-19 Tests May Help Early Identification of B.1.1.7, <https://www.thermofisher.com/blog/ask-a-scientist/the-s-gene-advantage-taqpath-covid-19-tests-may-help-early-identification-of-b-1-1-7/>. (Accessed, Jan 2. 2022).
- [13] Cepheid, Xpert Xpress CoV-2/Flu/RSV plus, [https://www.cepheid.com/en\\_US/tests/Critical-Infectious-Diseases/Xpert-Xpress-CoV-2-Flu-RSV-plus#product-resources](https://www.cepheid.com/en_US/tests/Critical-Infectious-Diseases/Xpert-Xpress-CoV-2-Flu-RSV-plus#product-resources), (Accessed, Jan 2. 2022).
- [14] X. Zhu *et al.*, “Multiplex reverse transcription loop-mediated isothermal amplification combined with nanoparticle-based lateral flow biosensor for the diagnosis of COVID-19,” *Biosens. Bioelectron.*, vol. 166, no. May, p. 112437, 2020, doi: 10.1016/j.bios.2020.112437.
- [15] D. C. Nyan and K. L. Swinson, “A novel multiplex isothermal amplification method for rapid detection and identification of viruses,” *Sci. Rep.*, vol. 5, no. December, pp. 1–9, 2015, doi: 10.1038/srep17925.
- [16] M. Inaba *et al.*, “Diagnostic accuracy of LAMP versus PCR over the course of SARS-CoV-2 infection,” *Int. J. Infect. Dis.*, vol. 107, pp. 195–200, 2021, doi: 10.1016/j.ijid.2021.04.018.
- [17] C. Amaral *et al.*, “A molecular test based on RT-LAMP for rapid, sensitive and inexpensive colorimetric detection of SARS-CoV-2 in clinical samples,” *Sci. Rep.*, vol. 11, no. 1, pp. 1–12, 2021, doi: 10.1038/s41598-021-95799-6.
- [18] J. Moreno-Contreras *et al.*, “Saliva sampling and its direct lysis, an excellent option to increase the number of SARS-CoV-2 diagnostic tests in settings with supply shortages,” *J. Clin.*

- Microbiol.*, vol. 58, no. 10, pp. 1–6, 2020, doi: 10.1128/JCM.01659-20.
- [19] C. Ambrosi *et al.*, “SARS-CoV-2: Comparative analysis of different RNA extraction methods,” *J. Virol. Methods*, vol. 287, p. 114008, 2021, doi: 10.1016/j.jviromet.2020.114008.
- [20] A. Ganguli *et al.*, “Rapid isothermal amplification and portable detection system for SARS-CoV-2,” *Proc. Natl. Acad. Sci. U. S. A.*, vol. 117, no. 37, pp. 22727–22735, 2020, doi: 10.1073/pnas.2014739117.
- [21] A. Ganguli *et al.*, “Hands-free smartphone-based diagnostics for simultaneous detection of Zika, Chikungunya, and Dengue at point-of-care,” *Biomed. Microdevices*, vol. 19, no. 4, pp. 1–13, 2017, doi: 10.1007/s10544-017-0209-9.
- [22] D. R. E. Ranoa *et al.*, “Saliva-Based Molecular Testing for SARS-CoV-2 that Bypasses RNA Extraction,” *bioRxiv*, pp. 1–35, 2020, doi: 10.1101/2020.04.22.056283.
- [23] D. R. E. Ranoa *et al.*, “Mitigation of SARS-CoV-2 Transmission at a Large Public University,” *medRxiv*, p. 2021.08.03.21261548, 2021, [Online]. Available: <http://medrxiv.org/content/early/2021/08/05/2021.08.03.21261548.abstract>.
- [24] J. Rodriguez-Manzano *et al.*, “Handheld point-of-care system for rapid detection of SARS-CoV-2 extracted RNA in under 20 min,” *ACS Cent. Sci.*, vol. 7, no. 2, pp. 307–317, 2021, doi: 10.1021/acscentsci.0c01288.
- [25] U.S. Food and Drug Administration, ID NOW COVID - 19 - Letter of Authorization, <https://www.fda.gov/media/136522/download>, (Accessed, Jan 7. 2022).
- [26] U.S. Food and Drug Administration, Cue COVID - 19 Test for Home and Over The Counter (OTC) Use - Letter of Authorization, <https://www.fda.gov/media/146467/download>, (Accessed, Jan 7. 2022).
- [27] U.S. Food and Drug Administration, Lucira CHECK-IT COVID-19 Test Kit - Letter of Authorization, <https://www.fda.gov/media/147492/download>, (Accessed, Jan 7. 2022).
- [28] Centers for Disease Control and Prevention, Science Brief: Omicron (B.1.1.529) Variant, <https://www.cdc.gov/coronavirus/2019-ncov/science/science-briefs/scientific-brief-omicron-variant.html>, (Accessed, Jan 2. 2022).
- [29] R. L. Smith *et al.*, “Longitudinal Assessment of Diagnostic Test Performance Over the Course of Acute SARS-CoV-2 Infection,” *J. Infect. Dis.*, vol. 224, no. 6, pp. 976–982, 2021, doi: 10.1093/infdis/jiab337.
- [30] F. Sun *et al.*, “Smartphone-based multiplex 30-minute nucleic acid test of live virus from nasal swab extract,” *Lab Chip*, vol. 20, no. 9, pp. 1621–1627, 2020, doi: 10.1039/d0lc00304b.
- [31] A. Ganguli *et al.*, “Reverse Transcription Loop-Mediated Isothermal Amplification Assay for Ultrasensitive Detection of SARS-CoV - 2 in Saliva and Viral Transport Medium Clinical Samples,” 2021, doi: 10.1021/acs.analchem.0c05170.
- [32] X. Xie *et al.*, “Neutralization of SARS-CoV-2 spike 69/70 deletion, E484K and N501Y variants by BNT162b2 vaccine-elicited sera,” *Nat. Med.*, vol. 27, no. April, 2021, doi: 10.1038/s41591-021-01270-4.
- [33] Y. Zhang, G. Ren, J. Buss, A. J. Barry, G. C. Patton, and N. A. Tanner, “Enhancing colorimetric loop-mediated isothermal amplification speed and sensitivity with guanidine chloride,” *Biotechniques*, vol. 69, no. 3, pp. 179–185, 2020, doi: 10.2144/btn-2020-0078.
- [34] J. R. Tumbleston *et al.*, “Continuous liquid interface production of 3D objects,” *Science (80-. )*, vol. 347, no. 6228, pp. 1349–1352, 2015, doi: 10.1126/science.aaa2397.
- [35] N. Li *et al.*, “Overcoming the limitations of COVID-19 diagnostics with nanostructures, nucleic acid engineering, and additive manufacturing,” *Curr. Opin. Solid State Mater. Sci.*, vol. 26, no. 1, 2022, doi: 10.1016/j.cossms.2021.100966.
- [36] H. De Puig *et al.*, “Minimally instrumented SHERLOCK (miSHERLOCK) for CRISPR-based point-of-care diagnosis of SARS-CoV-2 and emerging variants,” *Sci. Adv.*, vol. 7, no. 32, pp. 23–26, 2021, doi: 10.1126/sciadv.abh2944.

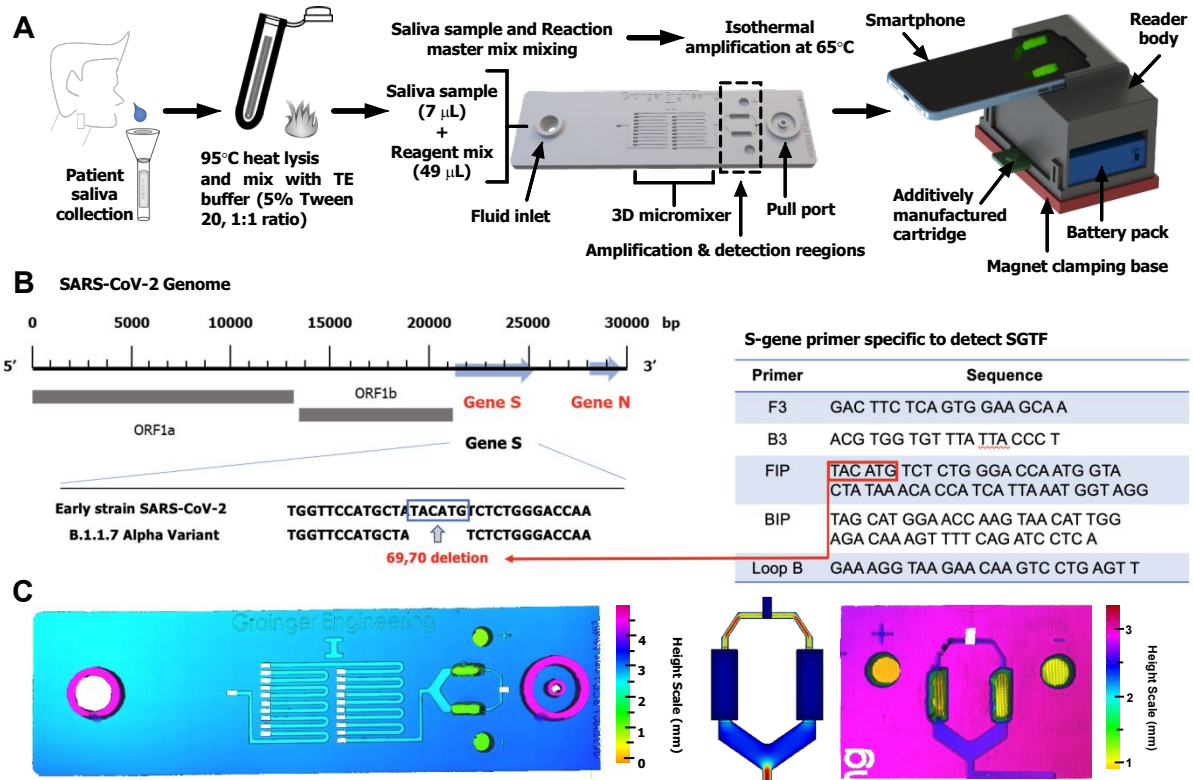


**Fig. 1.** Point-of-care device for SARS-CoV-2 detection from saliva samples. (A) Protocol workflow from saliva collection to the on-cartridge detection. (B) SARS-CoV-2 genome map highlighting detection regions. Two multiplexed assays were developed: one assay use two primer sets to detect the N- and S-gene in the early strains and the other assay use two primer sets to detect the N- and S-gene in the Alpha variant using the SGTF. (C) Detail of the additively manufactured microfluidic cartridge.

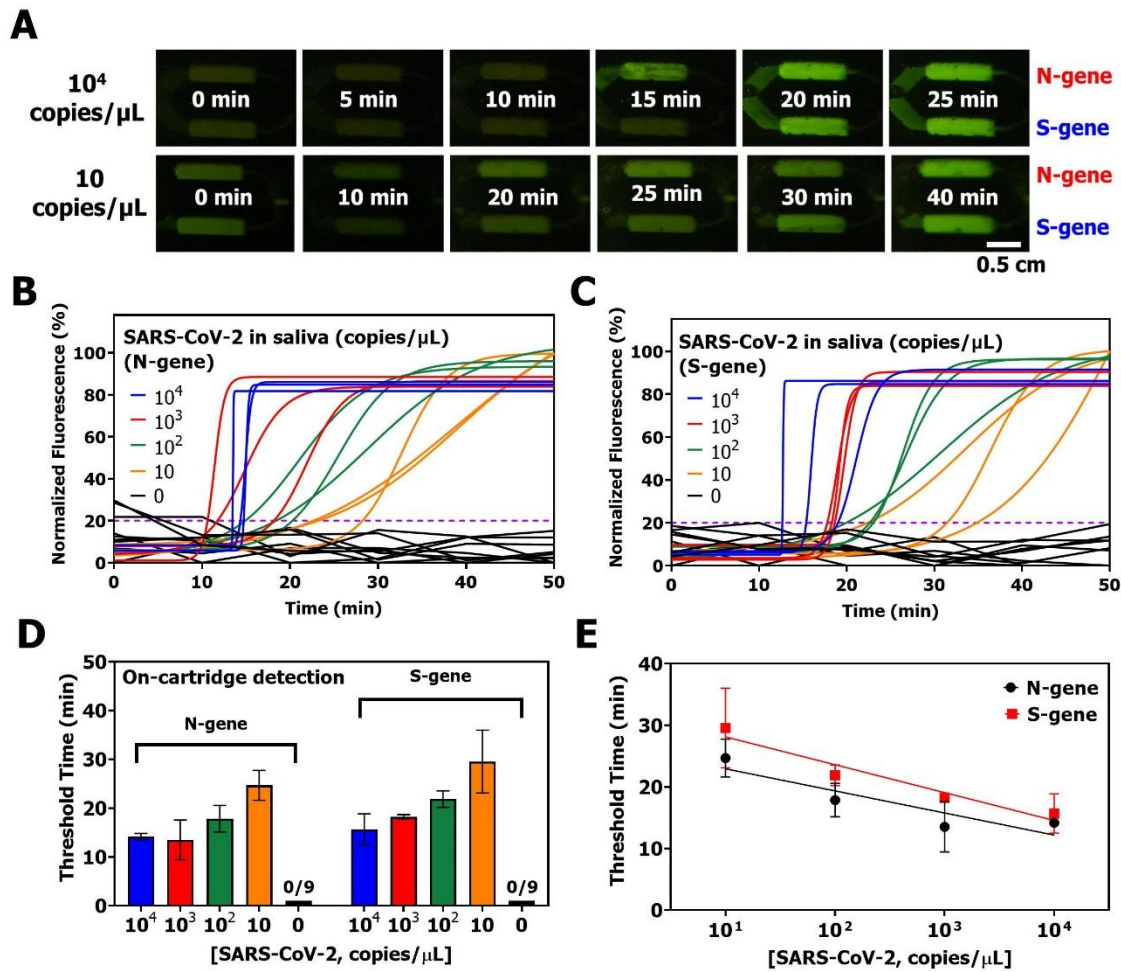


**Fig. 2.** On-cartridge detection of inactivated SARS-CoV-2 virus spiked in saliva using an additively manufactured cartridge and a handheld POC device. (A) Fluorescence images of the real-time RT-LAMP reaction (65°C, 50 min.) for multiplexed detection (N- and S-genes). The pre-dehydrated primers allowed the simultaneous detection of the two target genes in a single cartridge (upper detection region for N-gene and lower detection region for S-gene). Scale bar = 0.5 cm. (B-C) Normalized fluorescence amplification curves ( $n = 3-9$ ) for SARS-CoV-2 detection, (B) N-gene and (C) S-gene, from spiked saliva samples. (D) Amplification threshold time calculated at 20% of fluorescence signal. (E) Calibration curves for SARS-CoV-2 detection (N- and S-gene) spiked in saliva.

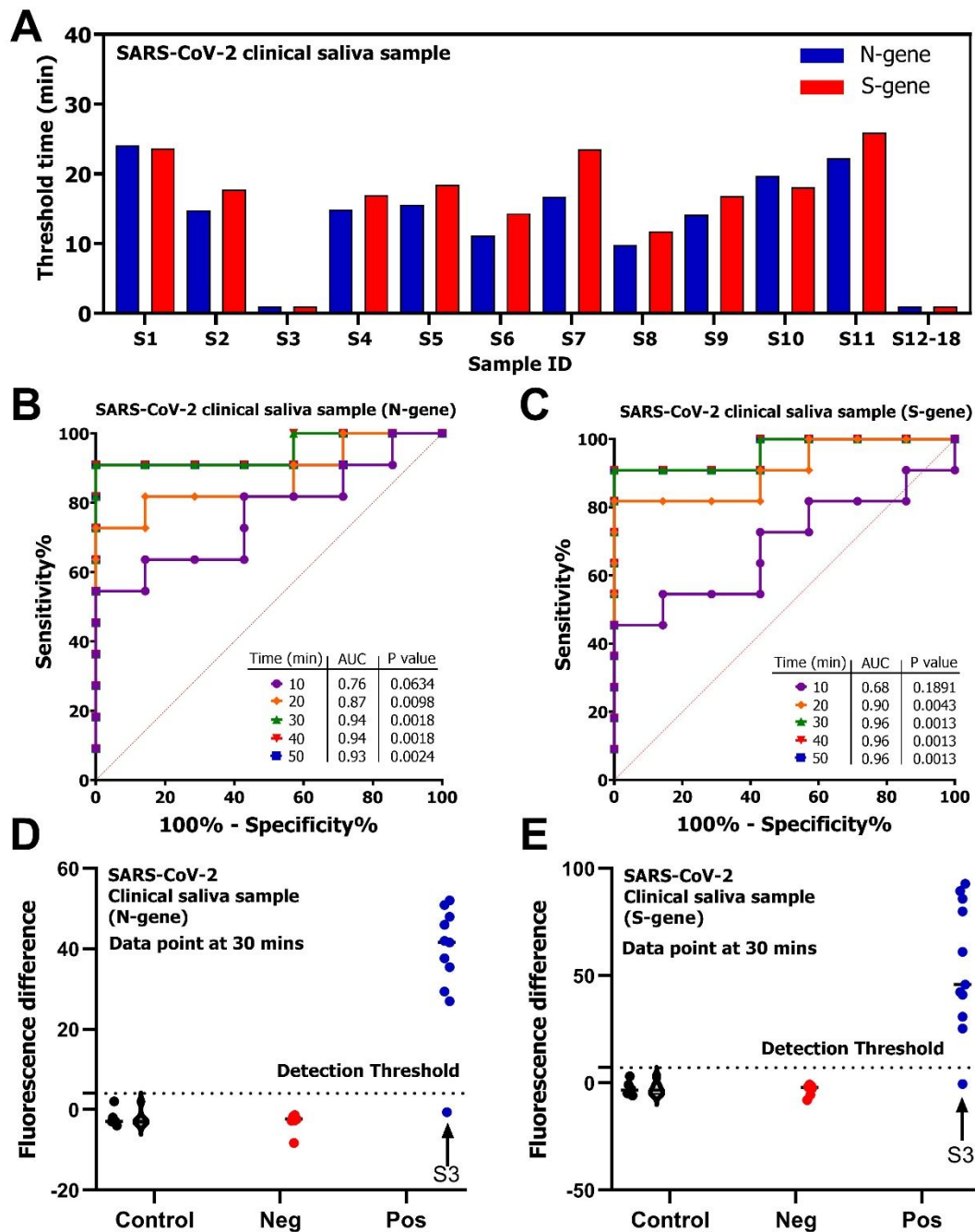


**Fig. 3.** On-cartridge detection of SARS-CoV-2 clinical saliva samples using an additively manufactured cartridge and a handheld POC device. The pre-dehydrated primers allowed the simultaneous detection of the two target genes in a single cartridge (A) Amplification threshold time results of 18 clinical samples calculated at 20% of the normalized fluorescence signal. ROC curves analyzed at five different time points for (B) N-gene and (C) S-gene. Based on the data points at 30 mins, discerning criterion to differentiate positive from negative samples for amplification of the (D) N-gene and (E) S-gene. Results obtained from the clinical samples were compared with a created baseline (using 6 known negatives samples). Detection threshold was calculated using the value of the average +  $3\sigma$  of blank controls (black dots for the raw data, grey for violin plot). Samples with fluorescence intensity above the detection threshold were considered as positive (blue dots), while samples with fluorescence intensity below the detection threshold were considered as negative (red dots).

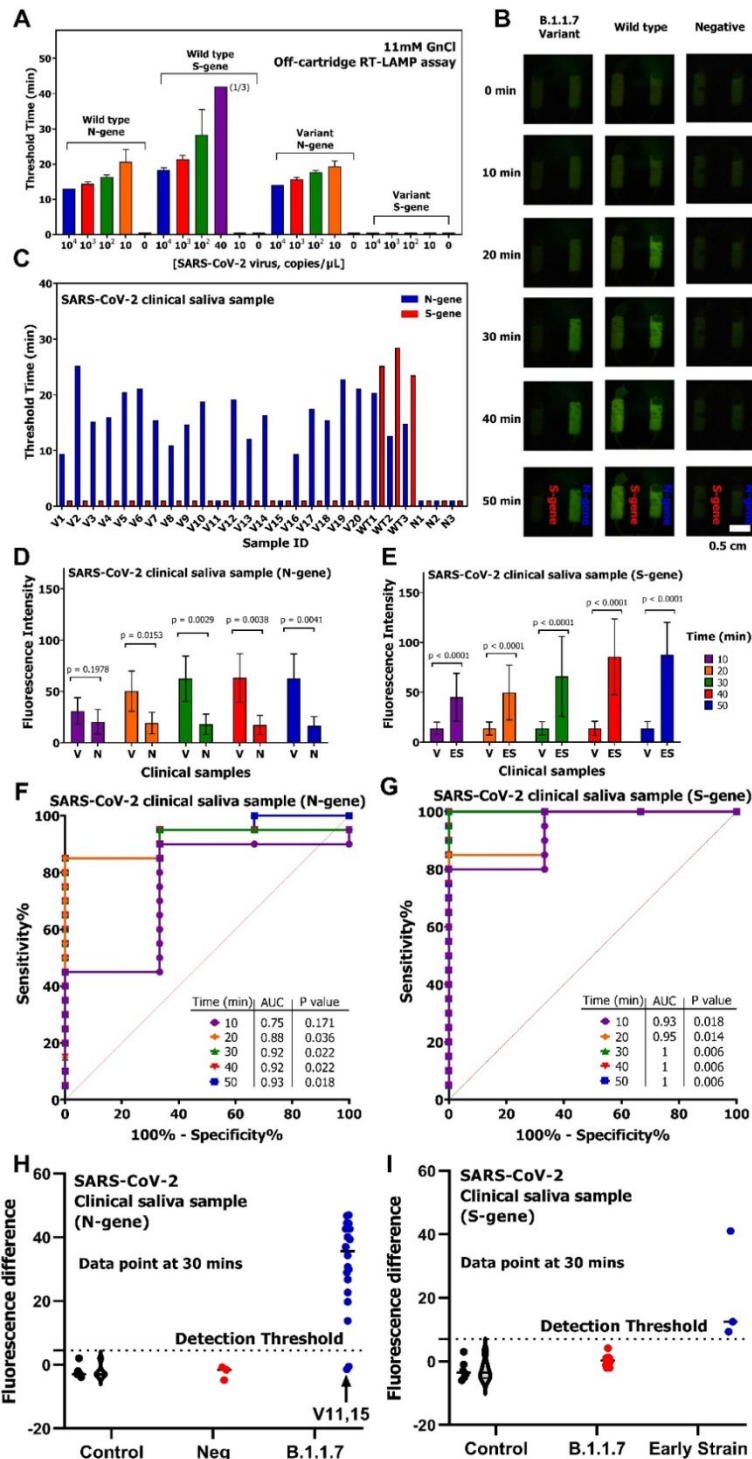


**Fig. 4.** Detection of B.1.1.7 variant samples and differentiation from the negative and early strains virus samples. (A) Off-cartridge sensitivity characterization of the GnCl RT-LAMP assay. Both the N- and S-gene primers specific to detect the SGTF were tested with early strains and B.1.1.7 variant viruses spiked in saliva samples. (B) On-cartridge images to distinguish the SARS-CoV-2 early strains from the B.1.1.7 variant. N-gene primer set, and S-gene primer set (specific to SGTF) are pre-dehydrated in the upper and lower detection region, respectively. Scale bar = 0.5 cm. (C) Amplification threshold times for 26 clinical saliva samples (20 B.1.1.7 variant, 3 early strains and 3 negative samples). Statistical comparison between (D) B.1.1.7 variant (V) and negative samples (N) and (E) B.1.1.7 variant and early strains (ES) samples. ROC curves summarizing the diagnostic ability to (F) detect the B.1.1.7 variant and (G) differentiate it from early strains samples. Based on the data points at 30 mins, discerning criterion (H) to differentiate B.1.1.7 variant from negative samples using the amplification of the N-gene and (I) to differentiate B.1.1.7 variant from the SARS-CoV-2 early strains using the amplification of the S-gene specific to SGTF.